Clim. Past Discuss., 7, 3489–3509, 2011
www.clim-past-discuss.net/7/3489/2011/
doi:10.5194/cpd-7-3489-2011

Climate
of the Past
Discussions

Role of CO_2 and Southern Ocean winds in glacial abrupt climate change

R. Banderas[1,2], **J. Álvarez-Solas**[1,2], **and M. Montoya**[1,2]

[1]Dpto. Astrofísica y Ciencias de la Atmósfera, Universidad Complutense, Madrid, Spain
[2]Instituto de Geociencias (UCM-CSIC), Madrid, Spain

Received: 4 October 2011 – Accepted: 18 October 2011 – Published: 20 October 2011

Correspondence to: R. Banderas (banderas.ruben@fis.ucm.es)

Published by Copernicus Publications on behalf of the European Geosciences Union.

Abstract

The study of Greenland ice cores revealed two decades ago the abrupt character of glacial millennial-scale climate variability. Several triggering mechanisms have been proposed and confronted against growing proxy-data evidence. Although the implication of North Atlantic deep water (NADW) formation reorganisations seems robust nowadays, their final cause remains unclear. Here, the role of CO_2 and Southern Ocean winds is investigated using a coupled model of intermediate complexity in an experimental setup designed such that the climate system resides close to a threshold found in previous studies. An abrupt surface air temperature (SAT) increase over the North Atlantic is simulated in response to increasing atmospheric CO_2 levels and/or enhancing southern westerlies. The simulated abrupt warming shows a similar pattern and amplitude over Greenland as registered in ice-core records of Dansgaard-Oeschger (D/O) events. This is accompanied by a strong Atlantic meridional overturning circulation (AMOC) intensification. The AMOC strengthening is found to be caused by a northward shift of NADW formation sites into the Nordic Seas as a result of an increase in sea surface salinity in the Northeastern Atlantic. The latter is caused by a northward retreat of the sea-ice front in response to higher temperatures. In this way, a new mechanism that is consistent with proxy data is identified by which abrupt climate change can be promoted.

1 Introduction

The last glacial period (ca. 110–10 kyr BP) was characterised by remarkable climatic instability on millennial timescales, mainly associated with so-called Dansgaard-Oeschger (D/O) events (Alley et al., 1999). These are considered to be the most pronounced abrupt climate changes of the past 110 kyr and manifested as rapid warmings in Greenland by more than 10 K on decadal timescales (e.g. Dansgaard et al., 1993) with widespread global climatic effects (Voelker and Workshop Participants, 2002). Both modeling and reconstruction efforts have contributed to increase our understanding of these glacial abrupt climate changes. The current paradigm is that these were caused by reorganisations of North Atlantic deep water (NADW) formation (Alley et al., 1999; Ganopolski and Rahmstorf, 2001). However, the causes of these reorganisations remain unknown. Model studies generally employ freshwater forcing in the North Atlantic to mimic D/O-like fluctuations (e.g. Ganopolski and Rahmstorf, 2001) but the ultimate source of such a forcing has not been identified. Alternatively, a Southern Ocean origin of abrupt climate changes has also been proposed. Enhanced surface freshwater fluxes (Weaver et al., 2003) and slowly varying background climate conditions in the Southern Ocean (Knorr and Lohmann, 2007) have been shown to be able to trigger an Atlantic meridional overturning circulation (AMOC) intensification leading to an abrupt warming in the North Atlantic.

Ice core data and marine sediment proxies suggest atmospheric CO_2 levels rose during the last glacial period coinciding with periods of halted NADW formation and reduced stratification in the Southern Ocean (Ahn and Brook, 2008). Such CO_2 variations are strongly correlated with Antarctic temperature, which shows an out-of-phase relationship between both hemispheres (Blunier and Brook, 2001), and predate abrupt warmings in Greenland associated with the largest D/O events. In addition, recent biogenic opal reconstructions suggest that during deglaciation, as well as throughout the last glacial period, CO_2 rises were preceded by an increase in deep upwelling in the Southern Ocean (Anderson et al., 2009). Denton et al. (2010) and Toggweiler and Lea (2010) have proposed that the increase of both Southern Ocean upwelling and CO_2 levels was the consequence of a shift in atmospheric circulation patterns in response to a reduction of the AMOC through the so-called bipolar seesaw effect (Crowley, 1992; Stocker, 1998). Southern Ocean winds appear to have strengthened and shifted southward at the end of the last glacial period as well as during extreme cold periods in the Northern Hemisphere (Toggweiler, 2009). A southward shift of the intertropical convergence zone (ITCZ) and Southern Ocean winds can also take place via atmospheric teleconnections in response to a cooling in the North Atlantic as suggested by models (Lee et al., 2011).

Southern Ocean winds are one of the main driving factors of the AMOC (Kuhlbrodt et al., 2007). Thus, increased Southern Ocean westerlies could have led to an AMOC strengthening through the so-called Drake Passage effect (Toggweiler and Samuels, 1995). On the other hand, the concomitant effect of increasing atmospheric CO_2 levels on the glacial AMOC has not yet been assessed. Here, the former studies are taken together to investigate the effect of CO_2 and Southern Ocean winds variations on the glacial AMOC.

2 Model and experimental design

The model used in this study is CLIMBER-3*α* (Montoya et al., 2005). Its atmospheric component is a 2.5-dimensional statistical-dynamical model based on the assumption of a universal vertical structure of temperature and humidity in the atmosphere with a horizontal resolution of $7.5^\circ \times 22.5^\circ$ (Petoukhov et al., 2000). Its oceanic component contains the state-of-the-art Geophysical Fluid Dynamics Laboratory (GFDL) MOM-3 ocean general circulation model, with a horizontal resolution of 3.75° and 24 variably spaced vertical levels, and the ISIS thermodynamic-dynamic snow and sea-ice model (Fichefet and Maqueda, 1997). CLIMBER-3*α* satisfactorily describes the large-scale characteristics of the atmosphere, ocean and sea-ice on seasonal and longer timescales.

The present study builds upon a previous climate simulation of the Last Glacial Maximum (LGM, ca. 21 kyr BP; Montoya and Levermann, 2008). Boundary conditions followed the specifications of the Paleoclimate Modeling Intercomparison Project Phase II (PMIP2), namely: changes in insolation, a reduced equivalent atmospheric CO_2 concentration of 167 ppmv to account for the lowered CH_4, N_2O and CO_2 concentrations, the ICE-5G ice-sheet reconstruction (Peltier, 2004), and land-sea mask changes plus a global increase of salinity by 1 PSU to account for the ~120 m sea-level lowering. Montoya and Levermann (2008) investigated the sensitivity of the glacial AMOC to wind-stress strength by integrating the CLIMBER-3*α* model to equilibrium with the

Title Page
Abstract | Introduction
Conclusions | References
Tables | Figures
◀| |▶
◀ ▶
Back | Close
Full Screen / Esc
Printer-friendly Version
Interactive Discussion

Trenberth et al. (1989) surface wind-stress climatology multiplied globally by varying factors $\alpha \in [0.5, 2]$. At $\alpha = \alpha_c \equiv 1.7$ a threshold, associated with a drastic AMOC increase of more than 10 Sv and a northward shift of NADW formation north of the Greenland-Iceland Scotland (GIS) ridge, was found. We hypothesise herein that the glacial AMOC is close to this threshold. However, because D/O events take place within Marine Isotopic Stage (MIS) 3 (ca. 60–27 kyr BP) rather than at the LGM, an equivalent atmospheric CO_2 level of 200 ppmv resulting from the higher CH_4, N_2O and atmospheric CO_2 concentrations registered during the former period (Schilt et al., 2010) has been imposed to mimic MIS3 climatic conditions. Consequently, the starting point for the experiments shown herein is the final equilibrium state of a control climate simulation with $\alpha = 1.65$ and an equivalent atmospheric CO_2 level of 200 ppmv, hereafter our stadial state.

Three transient experiments have been performed to test the AMOC sensitivity to CO_2 and wind forcings: a simulation combining both factors, a scenario considering CO_2 forcing only and, finally, a wind-only forced experiment (Fig. 1a and b). CO_2 forcing consists of a linear increase in CO_2 levels by 20 ppmv in 1000 yr, thus at the highest end of the CO_2 increase rates suggested by Ahn and Brook (2008) and recent climate carbon-cycle simulations (Bouttes et al., 2011). Wind forcing implies wind-stress over the latitudinal band of Drake Passage is linearly increased with a wind-amplification rate of 0.4 in 1000 yr. This increase is roughly consistent with results of a recent atmospheric model study in which cold conditions in the North Atlantic were shown to lead to an intensification of Southern Ocean winds by ~25 % (Lee et al., 2011).

3 Stadial to interstadial transition

Increasing CO_2 levels and wind strength lead to a gradual warming in the Nordic Seas area (Fig. 1c, black). After about 700 yr the system is found to cross a critical point leading to an abrupt temperature increase in the North Atlantic sector which is accompanied by a strong AMOC strengthening by more than 20 Sv (Fig. 1d). The simulated interstadial state is thus characterised by a more vigorous AMOC, deeper convective areas together with reduced sea-ice in the Nordic Seas, and a temperature increase of up to 10 K in the North Atlantic relative to the stadial state (Fig. 2).

In order to elucidate the mechanism behind this abrupt climate shift, we assess the precursors of the interstadial state. To this end, we analyse the climate system 30 years before the jump into the interstadial (450, 750, and 1550 yr after switching on the forcing for the CO_2-plus-wind, CO_2-only, and wind-only experiments, respectively), hereafter the transition stage (see Fig. 1c and d). We furthermore assess separately those simulations in which only CO_2 and only Southern Ocean winds were changed, respectively.

Under CO_2-only forcing conditions, an abrupt surface air temperature (SAT) increase of up to 4 K occurs in the Nordic Seas once CO_2 reaches a level of ca. 215 ppmv (Fig. 1c). At this point the AMOC remains almost unchanged (Fig. 1d). This first abrupt warming is related to widespread loss of sea ice in the Nordic Seas and the resumption of NADW formation, which eventually leads to a strong intensification of the AMOC.

Density variations in the Nordic Seas are thus analysed as a precursor for triggering the AMOC recovery. Surface density anomalies at the transition stage reveal significant changes over the North Atlantic with respect to the stadial state, notably over the Nordic Seas and Fennoscandian coast (Fig. 3a). Temperature and salinity contributions to density variations indicate the major density anomalies are related to changes in salinity (Fig. 3). The surface density evolution, which results in a gradual erosion of vertical stratification previous to the jump into the interstadial state, indeed strongly correlates with surface salinity contribution to density changes (Fig. 4).

To understand the causes behind these salinity changes, surface freshwater fluxes over the Nordic Seas region have been analysed. Northern summer freshwater flux anomalies closely correlate with surface salinity anomalies (Fig. 5a and b). The latter persist throughout the year, explaining the less clear relationship in winter and in the annual mean (Fig. 5c–f). The surface freshwater flux in the area is reduced by 0.59 m yr^{-1} (25 %) during summer, mostly due to a reduction in sea-ice melting by

$0.53\ \mathrm{m\,yr^{-1}}$ (Table 1). Rising temperatures related to increased CO_2 levels result in enhanced Nordic Seas sea-ice melting. By itself, this would lead to local widespread freshening. However, together with the Nordic sea-ice cover decline, a northward shift of the polar front takes place north of the Fennoscandian coast, especially during the summer months (Fig. 5a). As a consequence, sea-ice export into this region is strongly reduced, counteracting the effect of sea-ice melting, and resulting in local net negative freshwater flux anomalies.

Increased CO_2 levels translate into a modest radiative forcing of about $0.35\ \mathrm{W\,m^{-2}}$ which leads to warming in the Nordic Seas by about 1 K (Fig. 1c) and, thereby, impacts the sea-ice distribution in this region, especially its southernmost margins, by leading to a northward retreat of the polar front. This leads to enhanced surface salinity and thereby denser surface waters in the vicinity of the Fennoscandian coast, which eventually results in a strengthening of the AMOC in response to a resumption of NADW formation in open-water areas which were previously capped by sea-ice during the stadial state.

Within the wind-only forcing scenario, an abrupt SAT increase by 4 K is also found in the North Atlantic about 1650 yr after switching on the forcing. In this case, however, the increased temperatures at the transition stage over the area result from a significant AMOC intensification (Fig. 1c and d). Enhanced winds over the Southern Ocean lead to an increase in deep upwelling over the latitudinal band of Drake Passage. This results in stronger outcropping of isopycnals in the Southern Ocean, and thereby a reduction of the density of Antarctic Intermediate Water (AAIW, not shown) which translates into an increase of the Atlantic outflow (Schewe and Levermann, 2010) by nearly 2 Sv (Fig. 6a). As a result, northward heat transport by the Atlantic Ocean is intensified at almost all latitudes (Fig. 6b). This suggests the AMOC is initially reactivated from southern latitudes in contrast with the CO_2-only run, in which virtually no changes in the AMOC and heat transport are found prior to the onset of the interstadial state (Fig. 6). As a result, North Atlantic waters become warmer in response to a slightly more vigorous AMOC. Increased North Atlantic SATs related to enhanced northward heat transport driven by the AMOC result in melting of the Nordic sea-ice cover. The sea-ice polar front retreats to the north, which translates into reduced freshwater fluxes and thereby increased surface salinity in critical convective areas in the North Atlantic. Again, sea-ice changes related to surface salinity increase dominate freshwater flux balance over this area (Table 1). In this case the reduction in freshwater flux over the Fennoscandian coast is of 0.53 m yr^{-1}, of which 0.47 m yr^{-1} (∼90 %) are due to the sea-ice reduction. The resulting salinity anomalies are considered to be the precursors of NADW formation recovery leading to the interstadial state. Finally, combining CO_2 and wind forcings translates into a prompter climate response, suggesting both forcings work in the same sense to trigger an abrupt climate shift (Fig. 1).

4 Conclusions and discussion

We have investigated the climatic response to increasing atmospheric CO_2 levels and Southern Ocean winds when the glacial climate state is close to a threshold. Increasing CO_2 and Southern Ocean winds are both found to lead to an abrupt SAT increase over the Nordic Seas, resembling the large and rapid warmings associated with D/O events occurred during the last glacial period. The simulated abrupt warming is caused by reduced seasonal sea-ice southward export in the North Atlantic within the three forcing scenarios.

Our results are consistent with previous studies suggesting an important role of sea-ice in abrupt warming (Gildor and Tziperman, 2003; Li et al., 2005). Yet, in our simulations sea-ice retreat causes the initial abrupt SAT increase in response to the onset of convection in the Nordic Seas, but it is the AMOC intensification which helps to sustain the system in the warm state. Note despite the abruptness of the initial SAT increase, the AMOC response is more gradual, lasting several decades until the interstadial state is reached. Thus the fact that an abrupt response of the AMOC is not found does not preclude the latter playing an important role in abrupt climate change.

Despite the similarities in the Nordic Seas temperature response between these three scenarios, the mechanism behind the transition to the interstadial in the CO_2-only run is quite different from the experiment considering exclusively the wind amplification factor. In the CO_2-only simulation, the sea-ice retreat is mainly due to the increased temperatures following the enhanced CO_2. In contrast, in the wind-only run it is caused by higher temperatures due to a more vigorous heat transport from Southern latitudes in response to enhanced Southern Ocean winds.

The freshwater flux mechanism found herein is different from the salinity advection mechanism in the North Atlantic leading to a rapid AMOC switch-on described by Montoya and Levermann (2008). Note that in the latter study the model was integrated to the equilibrium by changing globally the oceanic wind-stress in different simulations. Within this context, enhanced surface wind-stress in the North Atlantic was found to increase the horizontal gyre circulation both in the subtropics and the subpolar regions, leading to enhanced salinity transport from the Tropics to the North Atlantic in the upper ocean layers. This mechanism is initially absent here. We investigate the climatic response by means of three transient experiments in which only the Southern Ocean wind-stress and/or the CO_2 concentration are varied. Note that the precursors are analysed at the transition state, thus prior to the interstadial. By contrast, once a relatively large change in the AMOC is accomplished (i.e. once the interstadial state is fully reached), the northward salinity transport does increase considerably as analysed in Montoya and Levermann (2008).

Note that the current model setup has been chosen so that the system resides close to a threshold associated with drastic changes in the oceanic circulation. The existence and location of such thresholds are model dependent. In addition, it is conceivable that small perturbations of a different origin could cause a transition, assuming such perturbations are able to significantly affect density in the Nordic Seas area . Here, we have identified a mechanism which is consistent with proxy records by which abrupt climate change can be promoted through the idealised experiments exhibited. Up to now climate simulations focusing on abrupt climate changes have mainly been based on imposing freshwater fluctuations in the North Atlantic as reviewed by Kageyama et al. (2010). However, the sources of these freshwater fluxes have not yet been identified. Recent studies point out the necessity to improve the ability of state-of-the-art models to simulate abrupt climate changes within the context of threshold values. This highlights the necessity to explore new research lines of past forcing factors which may help to understand the ensuing climate response (Valdes, 2011; Stocker and Marchal, 2000). Here, we propose such freshwater flux variations could be connected with rearrangements in the Nordic Seas sea-ice extent in response to CO_2 and Southern Ocean wind intensifications. Our results could be reassessed with more comprehensive models in the future.

Models and data indicate that wind and CO_2 increases are themselves the response to a previous North Atlantic cooling leading to a reorganisation of Southern Ocean and southward shift of the wind pattern (Chiang and Bitz, 2005; Lee et al., 2011). The oceanic explanation is that during stadial conditions, northward oceanic heat transport is strongly diminished in response to a weak overturning. As a consequence, the Southern Hemisphere warms at expense of the Northern Hemisphere through the bipolar seesaw effect. The temperature asymmetry is thereby reduced and the ITCZ and the large pressure circulation patterns shift to the south (Denton et al., 2010; Toggweiler and Lea, 2010). Alternatively, atmospheric models also indicate a southward shift of the intertropical convergence zone (ITCZ) and Southern Ocean winds can take place via atmospheric teleconnections in response to a cooling in the North Atlantic (Lee et al., 2011). Regardless of the exact causes, in this situation Southern Ocean westerlies are better aligned with the Antarctic Circumpolar Current (ACC). Within these conditions, atmospheric CO_2 levels increase in response to an oceanic upwelling intensification. According to our results, higher atmospheric CO_2 concentration and enhanced westerlies act to promote NADW formation over the Nordic Seas region through vital sea-ice variations. Thus, the AMOC is intensified and thereby the northward oceanic heat transport which eventually would translate into a northward shift of the ITCZ. At this point, Southern westerlies would progressively shift northward again, decreasing upwelling and atmospheric CO_2. This constitutes a negative feedback that favours the return into stadial conditions. As a conclusion this suggests that D/O events could be part of an internal oscillation which involves changes in CO_2, surface winds and AMOC on millennial timescales.

Acknowledgements. This work was funded by the Spanish Ministries for Environment (MARM) and Science and Innovation (MCINN) under the 200800050084028 and CGL08-06558-C02-01 projects. J. Álvarez-Solas was also funded by the Moncloa International Campus of Excellence (CEI). The model simulations were performed at the Spanish Environmental Research Centre (CIEMAT) in Madrid. We are also grateful to the PalMA group for useful comments and suggestions.

References

Ahn, J. and Brook, E.: Atmospheric CO_2 and climate on millennial time scales during the last glacial period, Science, 322, 83–85, doi:10.1126/science.1160832, 2008. 3491, 3493

Alley, R. B., Clark, P. U., Huybrechts, P., and Joughin, I.: The deglaciation of the Northern Hemisphere: a global perspective, Ann. Rev. Earth Planet Sci., 27, 149–182, doi:10.1146/annurev.earth.27.1.149, 1999. 3490, 3491

Anderson, R. F., Ali, S., Bradtmiller, L. I., Nielsen, S. H. H., Fleisher, M. Q., Anderson, B. E., and Burckle, L. H.: Wind-driven upwelling in the Southern Ocean and the deglacial rise in atmospheric CO_2, Science, 323, 1443–1448, doi:10.1126/science.1167441, 2009. 3491

Blunier, T. and Brook, E. J.: Timing of Millennial-Scale Climate Change in Antarctica and Greenland During the Last Glacial Period, Science, 291, 109–112, doi:10.1038/29447, 2001. 3491

Bouttes, N., Roche, D. M., and Paillard, D.: Systematic study of the fresh water fluxes impact on the carbon cycle, Clim. Past Discuss., 7, 1363–1392, doi:10.5194/cpd-7-1363-2011, 2011. 3493

Chiang, J. and Bitz, C.: Influence of high latitude ice cover on the marine Intertropical Convergence Zone, Clim. Dynam., 25, 477–496, doi:10.1007/s00382-00–0040-5, 2005. 3498

Crowley, T. J.: North Atlantic Deep Water cools the Southern Hemisphere, Paleoceanogr., 7, 489–497, doi:10.1029/92PA01058, 1992. 3491

Dansgaard, W., Johnsen, S., Clausen, H., Dahl-Jensen, D., Gundestrup, N., Hammer, C., Hvidberg, C., Steffensen, J., Sveinbjörnsdottr, A., Jouzel, J., and Bond, G.: Evidence for

Title Page
Abstract | Introduction
Conclusions | References
Tables | Figures
◀| |▶
◀ ▶
Back | Close
Full Screen / Esc
Printer-friendly Version
Interactive Discussion

general instability of past climate from a 250-kyr ice-core record, Nature, 364, 218–220, doi:10.1038/364218a0, 1993. 3490

Denton, G., Anderson, R., Toggweiler, J., Edwards, R., Schaefer, J., and Putnam, A.: The last glacial termination, Science, 328, 1652, doi:10.1126/science.1184119, 2010. 3491, 3498

Fichefet, T. and Maqueda, M. A. M.: Sensitivity of a global sea ice model to the treatment of ice thermodynamics and dynamics, J. Geophys. Res., 102, 12609–12646, doi:10.1029/97JC00480, 1997. 3492

Ganopolski, A. and Rahmstorf, S.: Rapid changes of glacial climate simulated in a coupled climate model, Nature, 409, 153–158, doi:10.1038/35051500, 2001. 3491

Gildor, H. and Tziperman, E.: Sea-ice switches and abrupt climate change, Philos. T. R. Soc. Lond., 361, 1935–1944, doi:10.1098/rsta.2003.1244, 2003. 3496

Kageyama, M., Paul, A., Roche, D., and Van Meerbeeck, C.: Modelling glacial climatic millennial-scale variability related to changes in the Atlantic meridional overturning circulation: a review, Quaternary Sci. Rev., 2931–2956, doi:10.1016/j.quascirev.2010.05.029, 2010. 3498

Knorr, G. and Lohmann, G.: Rapid transitions in the Atlantic thermohaline circulation triggered by global warming and meltwater during the last deglaciation, Geochem. Geophy. Geosy., 8, Q12006, doi:10.1029/2007GC001604, 2007. 3491

Kuhlbrodt, T., Griesel, A., Montoya, M., Levermann, A., Hofmann, M., and Rahmstorf, S.: On the driving processes of the Atlantic meridional overturning circulation, Rev. Geophys., 45, RG2001, doi:10.1029/2004RG000166, 2007. 3492

Lee, S., Chiang, J., Matsumoto, K., and Tokos, K.: Southern Ocean wind response to North Atlantic cooling and the rise in atmospheric CO_2: modeling perspective and paleoceanography implications, Paleoceanogr., 26, PA1214, doi:10.1029/2010PA002004, 2011. 3491, 3493, 3498

Li, C., Battisti, D., Schrag, D., and Tziperman, E.: Abrupt climate shifts in Greenland due to displacements of the sea ice edge, Geophys. Res. Lett., 32, L19702, doi:10.1029/2005GL023492, 2005. 3496

Montoya, M. and Levermann, A.: Surface wind-stress threshold for glacial Atlantic overturning, Geophys. Res. Lett., 35, L03608, doi:10.1029/2007GL032560, 2008. 3492, 3497

Montoya, M., Griesel, A., Levermann, A., Mignot, J., Hofmann, M., Ganopolski, A., and Rahmstorf, S.: The Earth System Model of Intermediate Complexity CLIM*BER*-3α. Part I: description and performance for present day conditions, Clim. Dynam., 25, 237–263, doi:10.1007/s00382–005–0044–1, 2005. 3492

Peltier, W.: Global glacial isostasy and the surface of the ice-age Earth- The ICE-5 G(VM 2) model and GRACE, Ann. Rev. Earth Planet Sci., 32, 111–149, doi:10.1146/annurev.earth.32.082503.144359, 2004. 3492

Petoukhov, V., Ganopolski, A., Brovkin, V., Claussen, M., Eliseev, A., Kubatzki, C., and Rahmstorf, S.: CLIMBER-2: a climate system model of intermediate complexity. Part I: model description and performance for present climate, Clim. Dynam., 16, 1–17, doi:10.1007/PL00007919, 2000. 3492

Schewe, J. and Levermann, A.: The role of meridional density differences for a wind-driven overturning circulation, Clim. Dynam., 34, 547–556, doi:10.1007/s00382-009-0572-1, 2010. 3495

Schilt, A., Baumgartner, M., Schwander, J., Buiron, D., Capron, E., Chappellaz, J., Loulergue, L., Schupbach, S., Spahni, R., Fischer, H., and Stocker, T.: Atmospheric nitrous oxide during the last 140,000 years, Earth Planet Sci. Lett., 300, 33–43, doi:10.1016/j.epsl.2010.09.027, 2010. 3493

Stocker, T. F.: The Seesaw Effect, Science, 282, 61–62, doi:10.1126/science.282.5386.61, 1998. 3491

Stocker, T. F. and Marchal, O.: Abrupt climate change in the computer: Is it real?, Proc. Natl. Acad. Sci. USA, 97, 1362–1365, doi:10.1073/pnas.97.4.1362, 2000. 3498

Toggweiler, J. R.: Shifting westerlies, Science, 323, 1434–1435, doi:10.1126/science.1169823, 2009. 3491

Toggweiler, J. R. and Lea, D.: Temperature differences between the hemispheres and ice age climate variability, Paleoceanography, 25, PA2212, doi:10.1029/2009PA001758, 2010. 3491, 3498

Toggweiler, J. R. and Samuels, B.: Effect of Drake Passage on the global thermohaline circulation, Deep-Sea Res., 42, 477–500, doi:10.1016/0967-0637(95)00012-U, 1995. 3492

Trenberth, K., Olson, J., and Large, W.: A Global Ocean Wind Stress Climatology based on ECMWF Analyses, Tech. Rep. NCAR/TN-338+STR, National Center for Atmospheric Research, Boulder, Colorado, USA, 1989. 3493

Valdes, P.: Built for stability, Nat. Geosci., 4, 414–416, doi:10.1038/ngeo1200, 2011. 3498

Voelker, A. and Workshop Participants: Global distribution of centennial-scale records for marine isotope stage (MIS) 3: a database, Quarternary Sci. Rev., 21, 1185–1212, doi:10.1016/S0277-3791(01)00139-1, 2002. 3490

Weaver, A. J., Saenko, O. A., Clark, P. U., and Mitrovica, J. X.: Meltwater Pulse 1A from Antarctica as a Trigger of the Bølling-Allerød Warm Interval, Science, 299, 1709–1713, doi:10.1126/science.1081002, 2003. 3491

Table 1. Surface freshwater fluxes balance in $\mathrm{m\,yr^{-1}}$ over the Nordic Seas (67.5° N–75° N, 4° W–7.5° E) for the stadial and the transition state, and for the difference between them (transition minus stadial) during summer months (June–August) for the CO_2 only and wind-only experiments (left and right, respectively). SFF: total vertical freshwater flux, decomposed in precipitation (PRC), evaporation (EVP), sea-ice melting or formation (SI). LAT: freshwater transport. Positive values indicate freshwater flux into the ocean and freshwater transport into the Nordic seas area.

		CO_2-only		wind-only	
	Stadial	Transition	Transition minus stadial	Transition	Transition minus stadial
SFF	2.35	1.76	−0.59	1.82	−0.53
PRC	0.22	0.23	0.01	0.23	0.01
EVP	−0.11	−0.18	−0.07	−0.18	−0.07
SI	2.24	1.71	−0.53	1.77	−0.47
LAT	−0.52	−0.70	−0.18	−0.57	−0.05

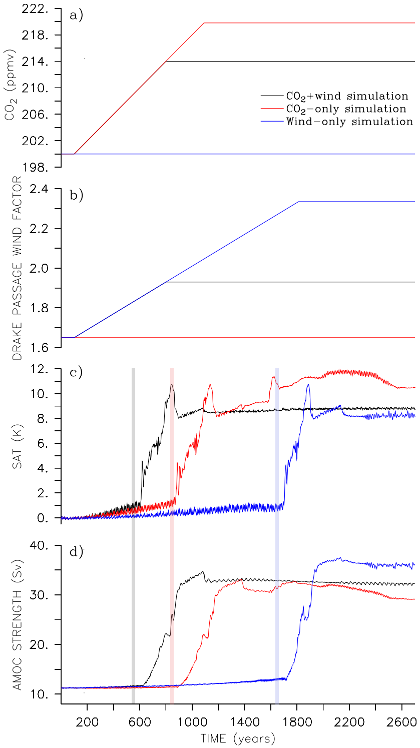

Fig. 1. Timeseries of forcings and relevant climatic variables: **(a)** CO_2 forcing in ppmv; **(b)** wind amplification factor over the Drake Passage (no units); **(c)** anomalies of North Atlantic SAT (67.5° N 11° W, in the Nordic Seas) with respect to the stadial state in K; **(d)** AMOC strength in Sv. Black, red and blue lines show the simulation combining CO_2 and wind forcings, the CO_2-only experiment, and the wind-only forced run, respectively. Black, red and blue shaded bars indicate the transition stages for the simulation combining CO_2 and wind forcings, the CO_2-only experiment and the wind-only forced run, respectively.

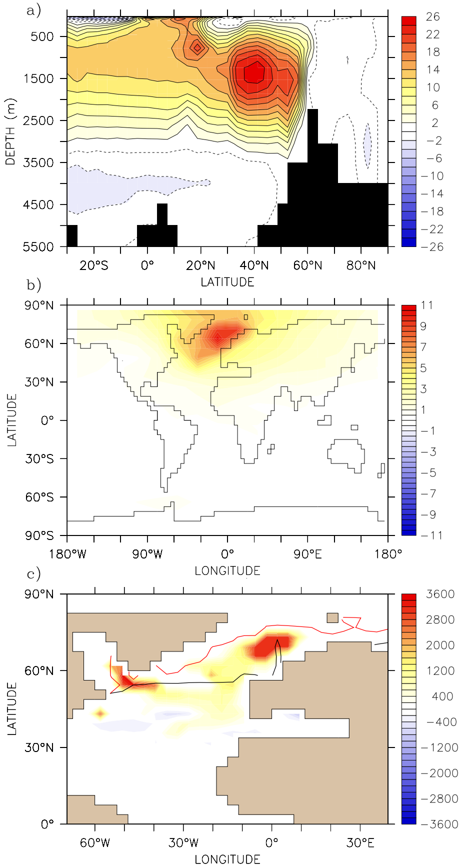

Fig. 2. Climatic patterns describing the interstadial state: **(a)** AMOC streamfunction in Sv; **(b)** SAT anomalies with respect to the stadial state in K; **(c)** interstadial minus stadial maximum convective depth differences in m. Black and red lines show the locations of the 90 % northern summer (June-August) average sea-ice concentration for the stadial and the interstadial regime, respectively.

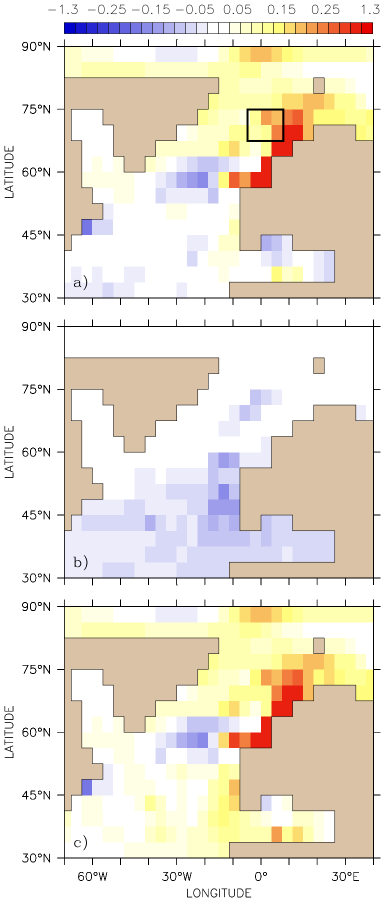

Fig. 3. Anomalies at the transition stage relative to the stadial regime for the CO_2-only experiment of **(a)** density; **(b)** temperature and **(c)** salinity contributions to density in $\mathrm{kg\,m^{-3}}$. The black box in **(panel a)** indicates the region where surface freshwater fluxes balance was calculated.

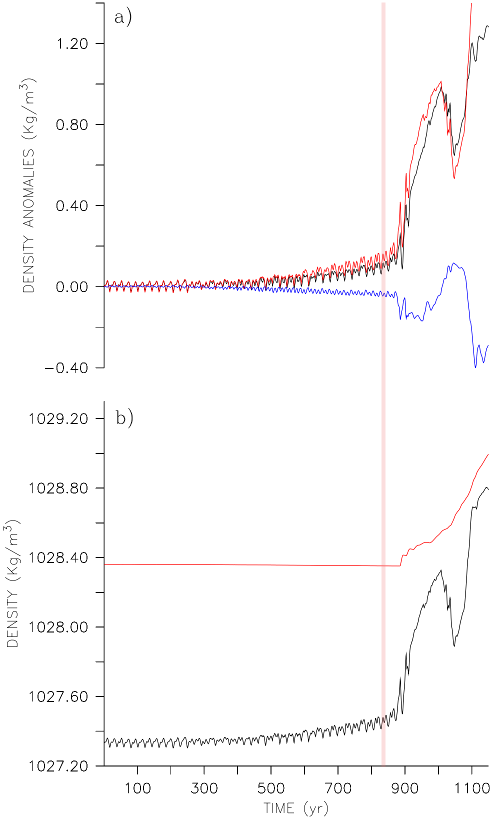

Fig. 4. (a) Surface anomalies with respect to the stadial state of density (black), together with salinity (red) and temperature (blue) contributions to density changes in kg m^{-3} over the Nordic Seas area (67.5° N–75° N, 4° W–7.5° E; black box in Fig. 3a); **(b)** density evolution over the same region at the surface (0–87.5 m; black line) and depth (2800 m; red line). The red shaded bar indicates the transition stage for the CO$_2$-only experiment.

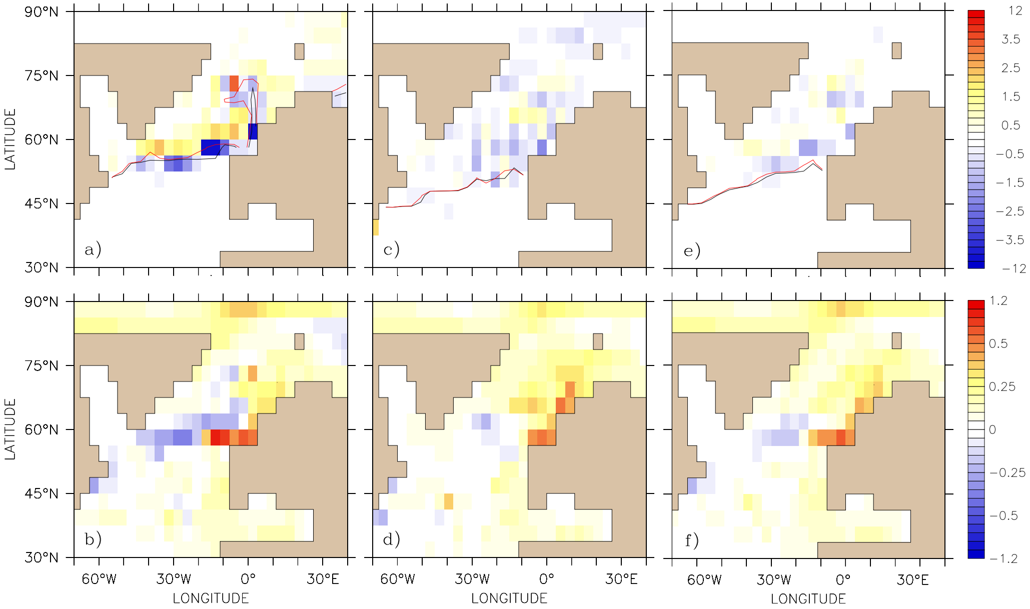

Fig. 5. Anomalies at the transition stage relative to the stadial regime under CO$_2$-only forcing conditions of **(a)** surface freshwater fluxes in m yr^{-1} and **(b)** surface salinity during summer months (June–August) in PSU; **(c–d)**, **(e–f)** same fields during winter (January–February) and for the annual mean, respectively. Black and red lines show the locations of the 90 % northern average sea-ice concentration for the stadial and the transition stage, respectively.

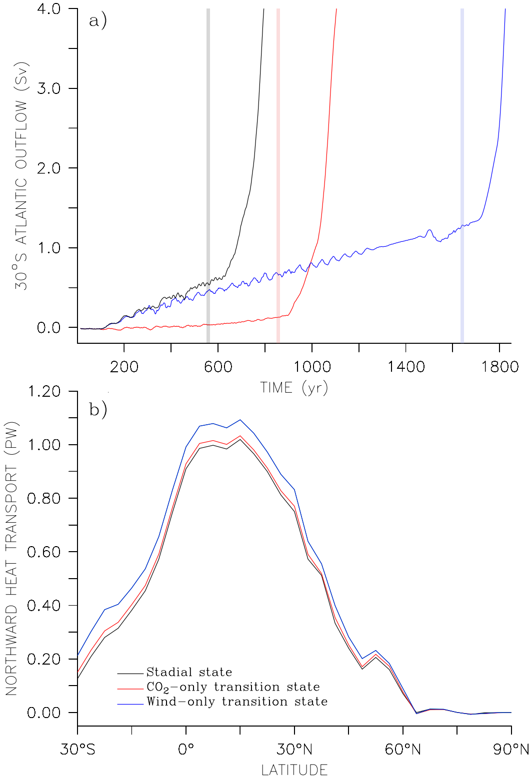

Fig. 6. (a) Evolution of AMOC outflow at 30° S in Sv for the CO$_2$-plus-wind simulation (black), CO$_2$-only (red) and wind-only (blue) forced experiments; **(b)** northward oceanic heat transport (0–1000 m depth) in PW for the stadial state (black) and transition stages for the CO$_2$-only (red) and wind-only (blue) forced experiments. Black, red and blue shaded bars indicate the transition stage for the simulation combining CO$_2$ and wind forcings, the CO$_2$-only run and the wind-only experiment, respectively.